AUTHOR(S):

Lim, Seonghyun; Kim, Taeyong; Yi, Sang-ri; Kim, Hyunjoong; Song, Junho

System-reliability-based Disaster Resilience Evaluation of Cable-stayed Bridge under Fire Hazard Using Reliability-Redundancy Analysis

Seonghyun Lim
Department of Civil and Environmental Engineering, Seoul National University, South Korea

Taeyong Kim
Department of Civil and Mineral Engineering, University of Toronto, Canada

Sang-ri Yi
Department of Civil and Environmental Engineering, University of California, Berkeley, USA

Hyunjoong Kim
School of Engineering, Liberty University, USA

Junho Song
Department of Civil and Environmental Engineering, Seoul National University, South Korea

ABSTRACT: The concept of disaster resilience recently emerged in efforts to gain holistic understanding of civil infrastructure systems exposed to various natural or human-made hazards. To effectively evaluate the resilience of complex infrastructure systems generally consisting of many interdependent structural components, Lim et al. (2022) proposed a system-reliability-based framework for disaster resilience. In the proposed framework, the disaster resilience of a civil infrastructure system is characterized by three criteria: reliability, redundancy, and recoverability. For comprehensive resilience analyses at the scale of individual structures, the reliability (β) and redundancy (π) indices were newly defined in the context of component- and system-level reliability analysis, respectively. Reliability-redundancy diagram, i.e., the scatter plot of the reliability and redundancy indices computed for each initial disruption scenario, was also proposed to help a decision-maker check whether the corresponding risk is acceptable for the society. In this paper, we demonstrate the framework through its application to a cable-stayed bridge in South Korea, the Seohae Grand Bridge under fire hazards. First, a probabilistic model is developed to describe the hazard of fire scenarios that may occur on the deck of the cable-stayed bridge. Next, finite element simulations are performed to compute the reliability and redundancy indices through component and system reliability analyses for the fire accident scenarios. An adaptive simulation method, AK-MCS (Echard et al. 2011), is employed to overcome the computational cost issue. The example successfully demonstrates that the reliability-redundancy analysis and diagram facilitate a comprehensive assessment of the disaster resilience of a complex civil infrastructure such as a cable-stayed bridge by using sophisticated computational simulations and advanced reliability methods.

1. INTRODUCTION

The societal risks caused by the inevitable exposures of civil infrastructure systems to various hazards have been escalating due to the increasing size and population density of urban areas. Structural systems are becoming more complex and larger as the technological demands from the complex urban societies increase rapidly. Accordingly, the uncertainties in hazard severity and the corresponding structural demands have been increased. It is thus intractable or impractical to secure the safety of every component in the target system against the risk caused by hazards. Consequently, the existing risk management frameworks aiming at preventing the failures of individual components has already revealed its fundamental limitations. As an alternative, the "resilience" concept is rapidly emerging as a future paradigm of disaster management based on a holistic understanding of the risk of the system failure instead of trying to prevent inevitable

component failures.

In such efforts regarding structural systems, the disaster resilience has been described by the functionality function and resilience triangle (Bruneau et al. 2003, Cimellaro et al. 2010). Further research has been conducted to evaluate resilience in a more refined and enhanced way, focusing on system functionality, the degree of degradation, and the speed of recovery after disaster-induced disruptions (Adams et al. 2012, Francis and Bekera 2014, Panteli et al. 2017, Zobel 2011). Though the various type of resilience measures were defined in existing studies, there is a limitation that system functionality function is usually characterized by a univariate function which cannot reflect the system aspect of civil engineering structures. Therefore, this functionality function-based approach may limit comprehensive understanding of component- and system-level performances of the structural system and their interactions.

To overcome this limitation, Lim et al. (2022) recently proposed to evaluate the disaster resilience of civil infrastructure systems from a viewpoint of system reliability analysis (Byun and Song 2017, Song et al. 2021). The proposed framework employs three criteria: reliability, redundancy, and recoverability. Among these criteria, the reliability (β) and redundancy (π) indices are mathematically defined to assess resilience comprehensively and develop a resilience-based risk measure. The "reliability-redundancy ($\beta-\pi$) diagram" is also introduced to provide a graphical method to assist disaster resilience evaluations, and risk-informed decision-making or optimization. This paper first reviews the proposed framework and demonstrates the applicability and effectiveness of the proposed disaster resilience framework for real-life complex structural systems through its application to a cable-stayed bridge under fire hazard. The numerical investigation employs an advanced reliability method for efficiency.

2. SYSTEM-RELIABILITY-BASED DISASTER RESILIENCE FRAMEWORK

2.1. *Three criteria of system-reliability-based disaster resilience: reliability, redundancy, and recoverability*

The proposed system-reliability-based framework characterizes the disaster resilience of a target civil infrastructure system, e.g., individual structure, lifeline network, urban community, in terms of three major criteria: reliability, redundancy, and recoverability (Lim et al. 2022). Figure 1 illustrates the criteria using a ball located near a cliff (inspired by metastability concept in physics) and two walls. The ball represents the target civil infrastructure system, which may start falling toward the cliff due to the indwelling hazards (represented by the purple arrow). The red wall visualizes the *reliability*, which is defined as "the capability of a component to avoid or minimize initial failures or disruptions despite the occurrence of a disastrous event." If components in the system are disrupted due to insufficient reliability, the system tries to "avoid or minimize cascading failures and degradation of system-level performance despite component-level disruption(s)" through its *redundancy* (blue wall). Finally, *recoverability* (yellow arrows) was defined as "the ability of engineers and society to take proper actions at components to recover the functionality of the system rapidly and completely." The three criteria provide a comprehensive understanding of the disaster resilience of a civil infrastructure system under external hazards with a focus on the relationship between the component disruptions and the system-level performance. The three criteria were discussed in detail at each of the three scales of civil infrastructure systems: individual structure, infrastructure network, and urban community, which led to a "3x3 resilience matrix."

Among the three scales, Lim et al. (2022) focused on the individual structure scale. For a structural system, the reliability and redundancy indices were defined using the results of component and system reliability analyses, as summarized in Section 2.2. These indices computed for the disruption scenarios of interest are visualized by a scatter plot termed reliability-redundancy

(β−π) diagram (Section 2.3), which can show the corresponding recoverability evaluated by socioeconomic studies.
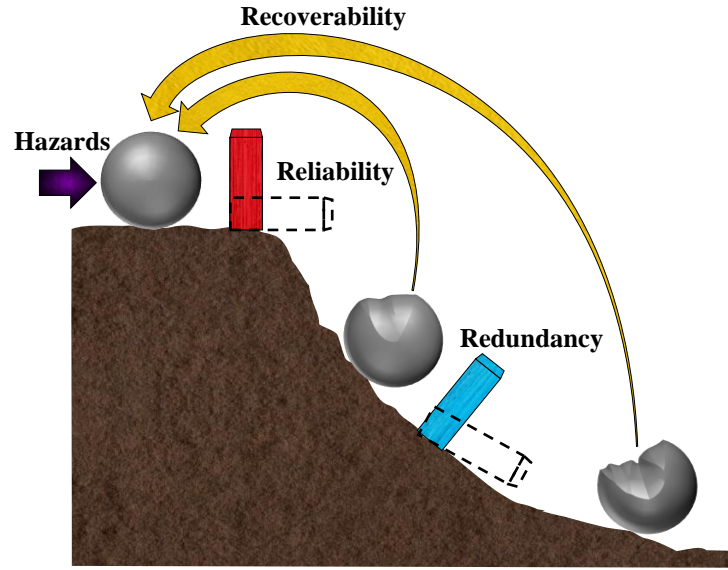
Figure 1 Three criteria of disaster resilience (Lim et al. 2022)

2.2. *Definitions of reliability (β) and redundancy (π) indices*

Following the aforementioned definition of the reliability criterion in the framework, the reliability index is defined in terms of the probability of i-th component failure event F_i given j-th hazardous event H_j as

$$\beta_{i,j} = -\Phi^{-1}\left(P\left(F_i|H_j\right)\right) \tag{1}$$

where $\Phi^{-1}(\cdot)$ denotes the inverse cumulative distribution function (CDF) of the standard normal distribution. A structural system exposed to hazards can experience various component failure events. Let us consider a system consisting of *n* components, each of which can be expressed with the Boolean states, e.g., fail and safe. Then, the number of initial component disruption events is $2^n - 1$. If the reliability index is calculated for each initial disruption scenario, the number of the reliability indices to be computed is identical to that of the initial disruption scenario. However, it is noted that highly unrealistic scenarios, e.g., every component failure except a single component, should not be considered for reliability calculation because their likelihoods are extremely low.

On the other hand, the redundancy index is defined in terms of the system failure probability given i-th component failure event F_i and j-th hazardous event H_j as

$$\pi_{i,j} = -\Phi^{-1}\left(P\left(F_{sys}|F_i, H_j\right)\right) \tag{2}$$

where F_{sys} denotes the system failure event. The redundancy index is also calculated for each of the initial component disruption scenarios. Thus, the number of acquired reliability-redundancy pairs is equal to that of the initial scenarios.

2.3. *Reliability-Redundancy (β−π) diagram and resilience limit-state surface*

The annual system failure probability caused by an initial disruption scenario can be obtained by multiplying the two conditional probabilities appearing in Eqs. (1) and (2) and the occurrence rate of j-th hazard λ_{H_j}, i.e.,

$$P(F_{sys,i,j}) = P(F_{sys}|F_i, H_j)P(F_i|H_j)\lambda_{H_j} = \Phi(-\pi_{i,j})\Phi(-\beta_{i,j})\lambda_{H_j} \qquad (3)$$

The objective of the proposed reliability-redundancy analysis is to check if the system failure probabilities are lower than *de minimis* risk (Ellingwood 2006), at which society does not call for any regulation, by

$$\Phi(-\pi_{i,j})\Phi(-\beta_{i,j})\lambda_{H_j} < P_{dm} \qquad (4)$$

where P_{dm} denotes the *de minimis* risk and generally has a value of 10^{-7} (Pate-Cornell 1994).

From Eq. (4), the resilience limit-state is identified in terms of β and π as

$$\frac{P_{dm}}{\lambda_{H_j}} - \Phi(-\pi_{i,j})\Phi(-\beta_{i,j}) = 0. \qquad (5)$$

After component- and system-reliability analyses for the initial disruption scenarios of interest, the corresponding β−π pairs are presented by a scatter plot termed β−π diagram, as shown in Figure 2 (left). The locations of the pairs are checked with respect to the resilience limit-state surface (for the occurrence rate of the hazard of interest, λ_{H_j}) from Eq. (5), as shown in Figure 2 (right). The pair inside the red zone is identified as the initial disruption scenario for which the disaster resilience should be improved to keep the risk lower than P_{dm}. Further decision-making process can be performed using the β−π diagram. The proposed process termed "reliability-redundancy (β−π) analysis" includes calculating β and π, obtaining the β−π diagram and the resilience limit-state surface, and identifying the scenarios which need further actions to improve the resilience, e.g., retrofits.
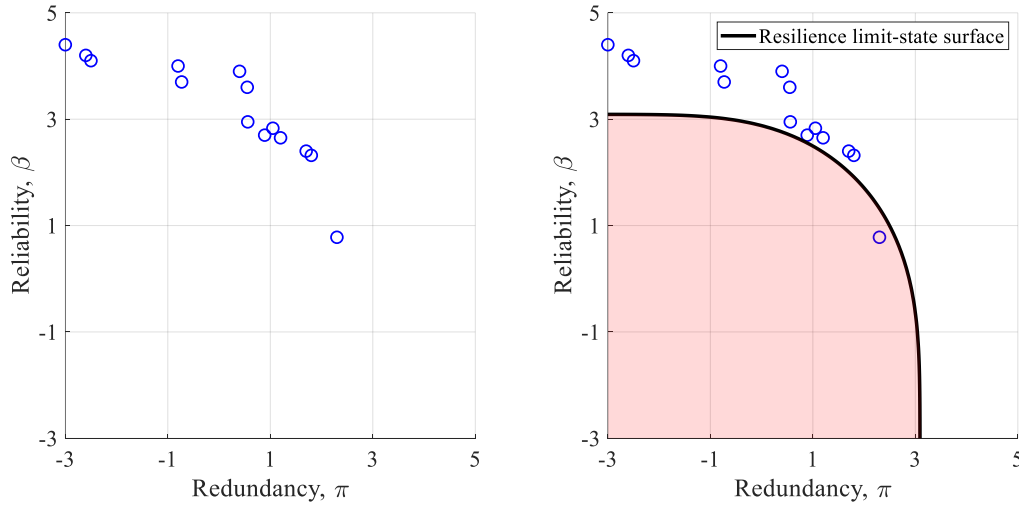

Figure 2 Example β−π diagram (Left), and the resilience limit state surface for the hazard occurrence rate $\lambda_{H_j} = 10^{-3}/yr$ shown in the diagram (Right)

3. RELIABILITY-REDUNDANCY (β−π) ANALYSIS OF CABLE-STAYED BRIDGE UNDER FIRE HAZARD

3.1. *Problem description*

In this study, we investigate a cable-stayed bridge example to demonstrate the applicability of the reliability-redundancy (β−π) analysis to real-life structural systems. To this end, the real-scale model of the Seohae Grand Bridge (Figure 3) is adopted to perform finite element component- and system-reliability analyses. The bridge has a 470-meter main span made of steel composite

and 144 steel cables. The hazard of interest is a tank-lorry accident in the shoulder lane, which may damage cable components through heat radiation.
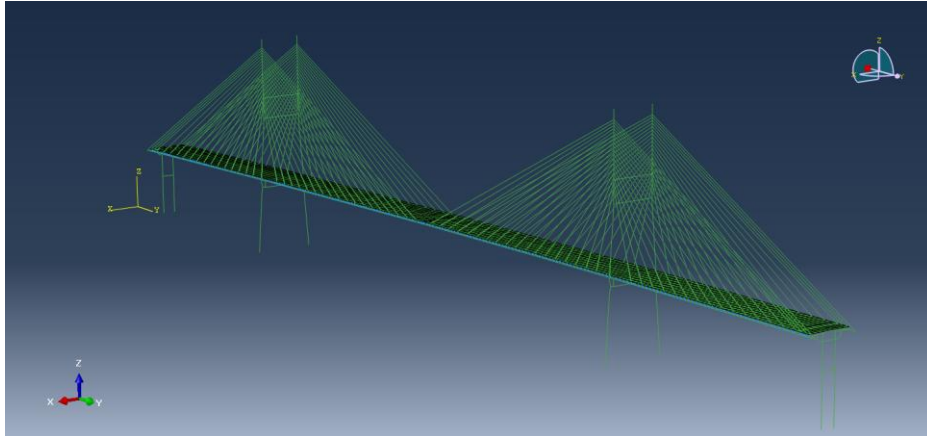

Figure 3 ABAQUS finite element model of Seohae Grand Bridge

3.2. *Probabilistic hazard modeling*

Because the cable-stayed bridge is located in an open space, it is assumed that heat generated from fire transfers to structure components only through radiation. To incorporate the uncertain factors of the hazard appropriately into the reliability analyses, we adopted the pool fire radiation model (Shokri and Beylor 1989). According to the model, the heat flux q'' for the given location and size of the fire can be predicted as

$$q'' = EF_{12} \tag{6}$$

where E denotes the effective emissive power and F_{12} refer to the configuration factor. The E has a high correlation with the diameter of the fire, D. On the other hand, the main factor determining the configuration factor F_{12} is the location of the fire. Therefore, in this study, the fire area A, the location of the fire, X, and the model error term $\sigma\epsilon$ of the D-E relationship are adopted as the random variables for the $\beta-\pi$ analysis. Figure 4 shows how the random variables propagate their uncertainty to the different elements in the fire model and the target variable q''. The obtained heat flux is transformed to the temperature of each cable and used as an input value for the finite element analyses.
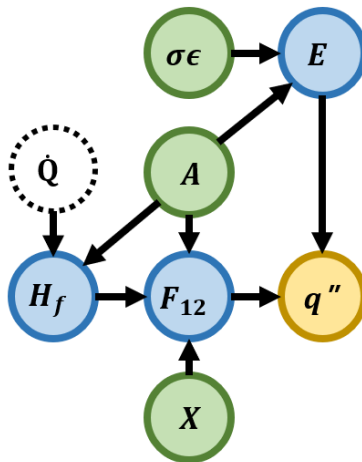
Figure 4 Relationships among the factors of the fire radiation model

3.3. *Reliability-Redundancy (β−π) analysis*

Before β−π analysis, the initial component disruption scenarios and the criterion of the system failure should be defined adequately. In this numerical investigation, it is assumed that the fire occurs on the deck of the cable-stayed bridge, thus, the cables are considered the most critical components of the superstructure during a fire accident. Therefore, the scenario of a single cable failure is considered an initial component disruption scenario. Moreover, the system failure is defined as the failures of two adjacent cables due to the load re-distribution. Accordingly, the limit-state functions for β and π calculations in Eqs. (1) and (2) are respectively set as:

$$g_\beta^i(\mathbf{x}) = \sigma_{yield}^i(\mathbf{x}) - \sigma_\beta^i(\mathbf{x}) \tag{7a}$$

$$g_\pi^i(\mathbf{x}) = \min \begin{pmatrix} \sigma_{yield}^{i+1}(\mathbf{x}) - \sigma_\pi^{i+1}(\mathbf{x}) \\ \sigma_{yield}^{i-1}(\mathbf{x}) - \sigma_\pi^{i-1}(\mathbf{x}) \end{pmatrix} \tag{7b}$$

where $g_\beta^i(\mathbf{x})$ indicates the limit-state function of the i-th cable failure, $g_\pi^i(\mathbf{x})$ denotes the limit-state function for the system failure event given i-th cable failure scenario, $\sigma_{yield}^i(\mathbf{x})$ is the yield stress of i-th cable, $\sigma_\beta^i(\mathbf{x})$ and $\sigma_\pi^i(\mathbf{x})$ represent the stresses of i-th cable as a result of FEM analysis in β and π calculations, respectively, and $\mathbf{x}$ is the vector of the random variables. Eq. (7b) indicates that the limit-state function is less than 0 when $(i + 1)$-th cable fails or $(i + 1)$-th cable fails. Considering the given initial event, i.e., i-th cable failure, this shows that the system failure is equal to the failure of two adjacent cables. In this example, using the fact that the Seohae Grand Bridge is symmetrical in both longitudinal and transverse directions, we can consider only 36 cables for the initial component disruption scenarios.

To obtain the β and π indices for the cable-stayed bridge, finite element analyses are performed for each realization of the fire random variables $\mathbf{x}$ using an ABAQUS® model developed for the Seohae Grand Bridge (see Figure 3). Monte Carlo simulation (MCS) is often used for simulation-based reliability methods, however, it is inefficient for cable-stayed bridge simulations due to expensive computational cost. For efficiency, this study adopted the active learning reliability method combining Kriging and Monte Carlo simulation (AK-MCS; Echard et al. 2011), which uses Kriging interpolations to approximate the limit-state function and finds the next sample point adaptively using a learning function for a more accurate surrogate model. Repeating this process until achieving a converged failure probability, one can obtain the failure probabilities for component- and system-reliability problems accurately and efficiently.
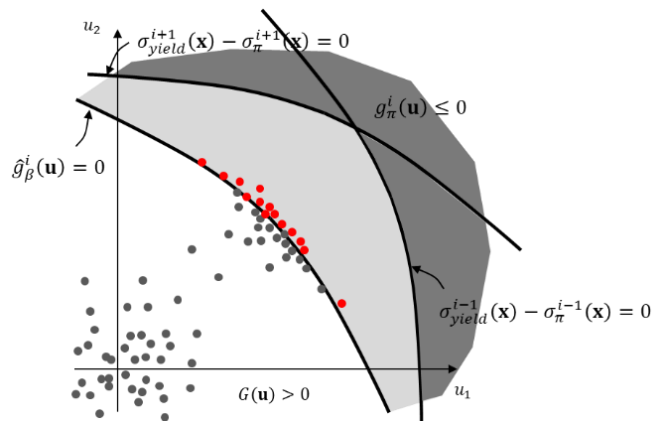

Figure 5 Relationship between the domains for reliability and redundancy calculations

There are several considerations we need to make for redundancy calculations. First, the sample space of system failure probability for redundancy calculation in Eq. (2) is more complex than

that for reliability calculation in Eq. (1), as shown in Figure 5. Therefore, for the best performance of AK-MCS during redundancy calculations, Monte Carlo points are sampled using Markov Chain Monte Carlo (MCMC) method. In this example, a total of 72 AK-MCS-based reliability analyses were performed for the 36 pairs of (β,π). We considered the physical coherence between the finite element models used for the reliability and redundancy calculations for the same initial disruption scenario. The coherence is simulated by considering the given initial component failure scenario as a condition in calculating the system failure probability. Accordingly, redundancy calculations should be able to incorporate the absence of failed components, load re-distributions, and the dynamic effects of component failures.

4. RESULTS OF RELIABILITY-REDUNDANCY (β−π) ANALYSIS

Through 72 repetitive AK-MCS-based reliability analyses, the β and π indices are obtained for each of the initial disruption scenarios defined as the failures of cables. The term $\Phi(-\pi_{i,j})\Phi(-\beta_{i,j})$ in Eq. (4), termed "per hazard *de minimis* risk (PHDMR)" can be also computed for each scenario. Figure 6 shows the reliability, redundancy, and PHDMR for each initial component disruption scenario plotted along with the structural configurations of the Seohae Grand Bridge. In the PHDMR plot (bottom), the horizontal red solid line indicates the threshold of PHDMR, i.e. P_{dm}/λ_H, with $\lambda_H = 10^{-3.8}/yr$. The scenarios whose PHDMR exceeds the resilience limit-state are represented by the cables in red color. These initial disruption scenarios that failed to meet the limit-state threshold also can be identified in the β−π diagram in Figure 7, which will be discussed below.
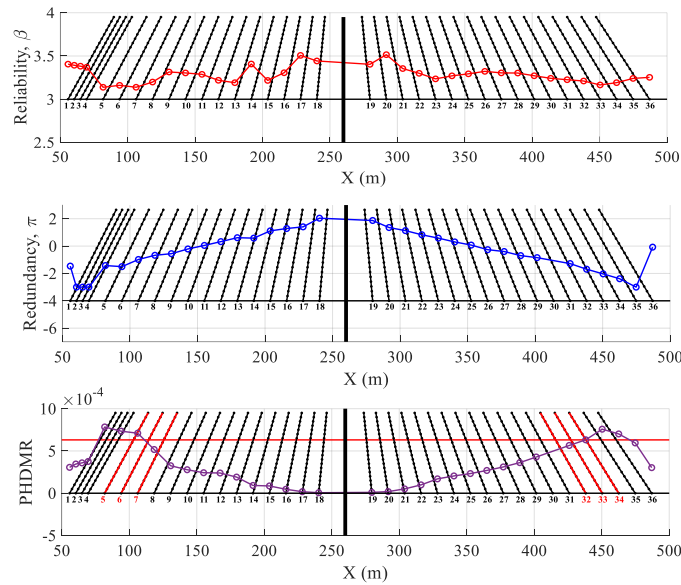

Figure 6 Reliability index (top), redundancy index (middle), and per hazard de minimis risk (bottom) obtained as a result of β−π analysis of the Seohae Grand Bridge under a fire hazard

Figure 7 shows the results of β−π analysis in the β−π diagram. The numbers shown beside the 36 β−π points indicate which cables failed in the corresponding scenarios. The black solid line is the resilience limit-state surface in Eq. (5) with an assumed hazard occurrence rate $\lambda_H = 10^{-3.8}/yr$. Based on this resilience limit-state surface, six points (representing the red-colored cables in Figure 6) failed to meet the target level of disaster resilience. For an example, if the initial disruption scenario of the fire-induced failure of the 33-th cable is considered, the Seohae Grand Bridge system has β of 3.166 and π of −2.032 at the corresponding initial failure

scenario. This combination does not satisfy the goal described in Eq. (4). This indicates that an action is needed to improve the disaster resilience of the bridge against the fire-induced failure at the cable.

The β–π diagram provides an intuitive presentation of the β–π analysis results. Moreover, it can support the decision-making process by identifying the scenarios requiring actions. For example, decision-makers may decide to retrofit the corresponding cables while considering recovery cost and other priorities. As discussed in Lim et al. (2022), the recoverability index can be calculated for each initial disruption scenario by socioeconomic studies and considered during the decision-making process and resilience-based decision optimization, for which further research is underway.
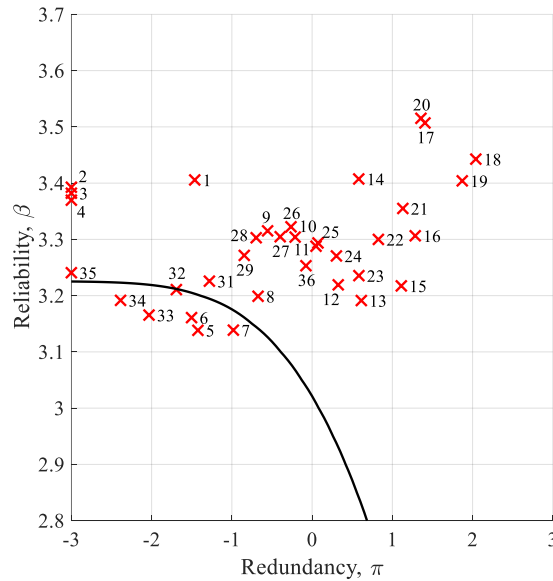
Figure 7 Reliability-Redundancy (β–π) diagram of the Seohae Grand Bridge under fire hazard

5. CONCLUSIONS

This study presented a system-reliability-based disaster resilience framework featuring three main criteria: reliability, redundancy, and recoverability for its applications to real-life complex structural systems. Based on the definitions of reliability and redundancy indices, the reliability-redundancy analysis method was delineated along with the resilience limit-state and the reliability-redundancy diagram. In the numerical example of a cable-stayed bridge under fire hazard, the fire hazard was probabilistically modeled and a finite element model was developed. To facilitate the reliability-redundancy analysis of the cable-stayed bridge, an active learning-based reliability method, named AK-MCS, was employed. The example successfully demonstrated the applicability and effectiveness of the proposed reliability-redundancy analysis and future research opportunities, e.g., methods to evaluate recoverability, resilience-based decision optimization.

ACKNOWLEDGEMENTS

REFERENCES

Adams, T.M., Bekkem, E., and Toledo-Durán, E.J. 2012. Freight resilience measures. *Journal of Transportation Engineering*. 138(11): 1403-1409.

Bruneau, M., Chang, S.E., Eguchi, R.T., Lee, G.C., O'Rourke, T.D., Reinhorn, A.M., Shinozuka, M., Tierney, K., Wallace, W.A., and von Winterfeldt, D. 2003. A Framework to quantitatively assess and enhance the seismic resilience of communities. *Earthquake Spectra*. 19 (4): 733-752.

Byun, J., and Song, J. 2017. Structural system reliability, reloaded. Chap. 2-2 in Risk and reliability analysis: Theory and applications. edited by P. Gardoni. Berlin. Springer.

Cimellaro, G.P., Reinhorn, A.M., and Bruneau, M. 2010. Framework for analytical quantification of disaster resilience. *Engineering Structures*. 32: 3639-3649.

Echard, B., Gayton, N., and Lemaire, M. 2011. AK-MCS: An active learning reliability method combining Kriging and Monte Carlo Simulation. Structural Safety. 33(2): 145-154.

Ellingwood, B.R. 2006. Mitigating risk from abnormal loads and progressive collapse. *Journal of Performance of Constructed Facilities*. 20(4): 315-323.

Francis, R., and Bekera, B. 2014. A metric and frameworks for resilience analysis of engineered and infrastructure systems. Reliability Engineering and System Safety. 121: 90-103.

Lim, S., Kim, T., and Song, J. 2022. System-reliability-based disaster resilience analysis: Framework and applications to structural systems. Structural Safety. 96: 102202.

Panteli, M., Mancarella, P., Trakas, D.N., Kyriakides, E., and Hatziargyriou, N.D. 2017. Metrics and quantification of operational and infrastructure resilience in power systems. IEEE Transactions on Power Systems. 32(6): 4732-4742.

Pate-Cornell, E. 1994. Quantitative safety goals for risk management of industrial facilities. *Structural Safety*. 13(3): 145–157.

Shokri, M., and Beyler, C.L. 1989. Radiation from Large Pool Fires. *Journal of Fire Protection Engineering*. 1(4): 141-150.

Song, J., Kang, W.-H., Lee, Y.-J., and Chun, J. 2021. Structural system reliability: overview of theories and applications to optimization. *ASCE-ASME Journal of Risk and Uncertainty in Engineering Systems, Part A: Civil Engineering*. 7(2): 03121001.

Zobel, C.W. 2011. Representing perceived tradeoffs in defining disaster resilience. *Decision Support Systems*. 50(2): 394-403.